Journal of Physics: Conference Series **420** (2013) 012141 doi:10.1088/1742-6596/420/1/012141

Searching for the low-energy resonances in the ^{12}C(^{12}C,n)^{23}Mg reaction cross section relevant for s-process nucleosynthesis

B Bucher, X Fang, S Almaraz-Calderon, A Alongi, A D Ayangeakaa, M Beard, A Best, J Browne, C Cahillane, M Couder, R deBoer, A Kontos, A Long, W Lu, S Lyons, M Notani, D Patel, N Paul, A Roberts, D Robertson, K Smith, E Stech, R Talwar, W Tan and X D Tang

Institute for Structure and Nuclear Astrophysics, Joint Institute for Nuclear Astrophysics, University of Notre Dame, Notre Dame, IN 46556, USA

E-mail: bbucher@nd.edu

Abstract. The ^{12}C(^{12}C,n) reaction (Q=-2.6 MeV) is a potential neutron source for the weak s-process occurring in shell-carbon burning of massive stars. The uncertainty in this reaction rate limits our understanding of the production of elements in the range $60 < A < 110$. Current stellar models must rely on the smooth extrapolation of a dubious statistical model calculation based on experimental data taken at energies well above the Gamow window which lies below 3.2 MeV. At Notre Dame, this reaction cross section has been measured in finer steps at energies above 3.5 MeV, while successful measurements down to 3.1 MeV have just recently been achieved. In addition, a new extrapolation based on measurements of the mirror system has been developed which predicts a number of low-energy resonances while accounting well for the high-energy resonances. An overview of this work along with the most recent results and astrophysical implications are presented.

1. Introduction

Most of the elements between iron and strontium are made in the weak s-process, which is thought to occur during the convective core-helium burning and convective shell-carbon burning phases of massive stars ($\gtrsim 8 M_\odot$)[1]. It is believed that the main source of neutrons for this process is the reaction ^{22}Ne(α,n)^{25}Mg, where the ^{22}Ne is made by successive α-captures on leftover ^{14}N from CNO hydrogen burning. The number of neutrons produced by this reaction is still somewhat uncertain, but must depend largely on the amount of ^{14}N prior to helium burning and the rate of ^{22}Ne(α,γ)^{26}Mg, which competes with the neutron channel [2]. All of the ^{22}Ne is expected to be exhausted by the early stages of shell-carbon burning. However, a potential secondary weak s-process may continue via the reaction ^{12}C(^{12}C,n)^{23}Mg occurring throughout the remainder of shell-carbon burning. Though this reaction is much slower than ^{22}Ne(α,n), the large abundance of carbon in the environment along with the high temperatures during shell burning may allow this channel to produce a significant neutron flux. Indeed, standard 1-D massive star models indicate that heavy element production in the carbon shell is sensitive to this reaction (see Fig.1). But in order to better understand the role of this

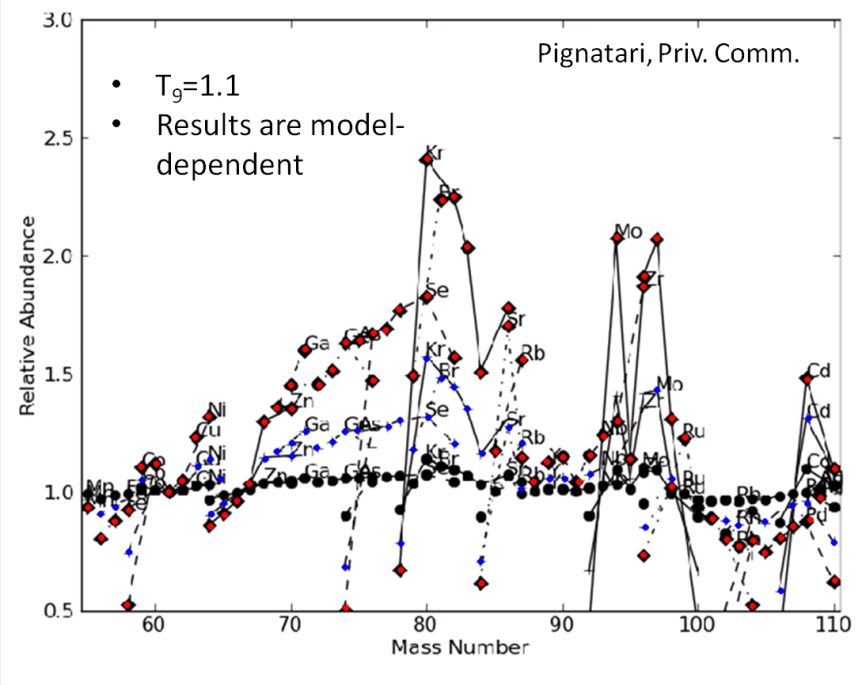

Figure 1. The changes in heavy element abundances produced in the carbon shell according to a 1-D stellar model of a 25$M_\odot$ solar metallicity star are shown after increasing the ^{12}C(^{12}C,n) rate by factors 2 (●), 5 (♦), and 10 (♦) [10].

reaction in the weak s-process, a more reliable reaction rate is needed. To date, this reaction is not well-studied, and the rate used in stellar models relies on an extrapolation of experimental data based on a renormalized statistical model calculation [3]. In that study, the ^{12}C(^{12}C,n) cross section was measured and the experimental neutron branching ratio was determined using the proton and alpha measurements in [4]. A Hauser-Feshbach statistical model was used to calculate the neutron branching ratio down to the reaction threshold at 2.6 MeV (center-of-mass). However, the calculation overpredicted the branching ratio by a factor of three compared with the experimental results, so the calculation was renormalized to fit the data. The resulting extrapolation is a smooth function, monotonically decreasing to zero at threshold, while the experimental excitation function is fluctuating, rich in structure, with a couple of resonances jumping high above the calculation. It is this resonant structure, observed in all exit channles of the ^{12}C+^{12}C fusion reaction [4–8], which makes the astrophysical rate so uncertain. Theory has yet to provide a successful model for this structure which exists down to the lowest measured energies. For ^{12}C(^{12}C,n) during shell-carbon burning ($T_9 \simeq 1.1$) the most important center-of-mass energies range between 2.8 and 3.2 MeV. The lowest cross section measurement to date is provided in [3] which stops at 3.54 MeV. However, even lower measurements exist for the proton and alpha channels (Fig.2). Interestingly, resonances have been observed within this energy range in the other channels [6, 8, 9]. Therefore, it would not be surprising to find corresponding resonances in the neutron channel contrary to the smooth extrapolation recommended in [3]. This work aims to verify these resonances using improved experimental techniques which allow the reaction cross section to be measured at lower energies. In addition, to cover the lowest energies inaccessible by experiment, an improved extrapolation technique is provided which is based on measurements of the mirror reaction ^{12}C(^{12}C,p)^{23}Na. The following sections describe two independent experimental techniques for measuring the ^{12}C(^{12}C,n)^{23}Mg cross section. The

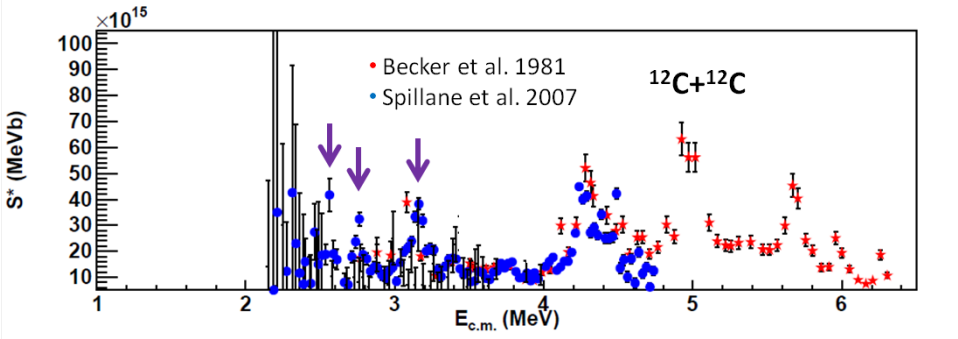

Figure 2. Astrophysical S* factor (S*(E)=S(E)$e^{0.46E}$, see [4] for details) is plotted for the combined proton and alpha channels of ^{12}C+^{12}C fusion with data from [8] ($\star$) and [6] ($\bullet$). The arrows ($\downarrow$) indicate resonances which occur at energies important for the neutron channel in the weak s-process.

first technique counts the β-decays of the residual ^{23}Mg (Sec. 2), while the second counts the evaporated neutrons directly (Sec. 4). Sec. 3 outlines the new extrapolation technique, and astrophysical implications and conclusions are given in Sec. 5 and 6 respectively.

2. ^{23}Mg decay measurement

This first measurement is similar to the methods of [3] and [4] in that it relies on the detection of the residual ^{23}Mg produced from the neutron channel of carbon fusion. It is especially similar to the method of [4] in that the β-rays are directly counted as a measure of ^{23}Mg production.

The experiment was performed at the University of Notre Dame's Nuclear Science Laboratory (NSL) where ^{12}C beams were accelerated by a 11 MV FN tandem Van de Graaff accelerator. A cesium-sputtering ion source was used to produce negative ^{12}C ions for injection into the tandem accelerator, while either a gas-stripping system or a thin carbon foil produced positive ions at the terminal, depending on the energy of the beam. A 90° dipole analyzing magnet was used to precisely select the beam energy and charge state of interest. A combination of electrostatic and magnetic steering and focusing elements guided the beam to a thin (20 μg/cm^2) carbon foil. A 5 cm diameter annular disk was placed 15 cm behind the target to catch the ^{23}Mg reaction products while the primary ^{12}C beam passed through a 5 mm hole in the center of the disk. Based on the geometric arrangement and the approximation of an isotropic center-of-mass angular distribution, it was estimated that 90% of the total ^{23}Mg produced was caught by the annular disk. The remaining 10% passed through the central hole with the beam and was not counted. The beam current was measured by a Faraday cup downstream from the catcher. Since the charge state of the beam ions was altered by passing through the target material, the Faraday cup reading required a normalization factor to scale back to the original charge state. This was measured for each beam energy by removing the target and allowing the beam to pass freely to the Faraday cup and comparing the two current readings.

As for the ^{23}Mg detection, after sufficient activity was collected on the catcher, it was moved by a motor-driven arm to a counting position adjacent to a 5 cm diameter plastic scintillator while the beam was blocked upstream of the target. Based on the ^{23}Mg half-life of 11.3 seconds, it was decided to allow 20 seconds of target irradiation and 40 seconds of counting time. This cycle was continuously repeated until enough counting statistics were obtained. Incident beam energies between 8 and 13 MeV were measured in increments of 100 keV (50 keV c.m.). The results are shown in Fig. 3. A few things are immediately apparent. The new data shows good agreement with the data from [3] and [4] in the overlapping regions, but the smaller step-

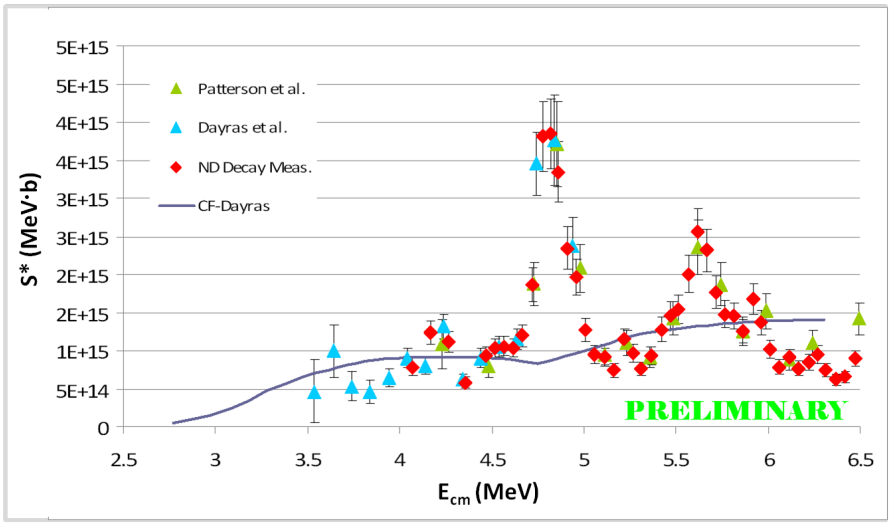

Figure 3. New data for ^{12}C(^{12}C,n) excitation function (♦) shown with previous data from [3] (▲) and [4] (▲). All three data sets display nice agreement. The curve (———) represents the calculation of S* based on the neutron branching ratio provided in [3] and the recommended total ^{12}C fusion S* provided in [12].

size provides a better map of the resonant structure in the excitation function. However, this measurement was unable to provide data down to the lowest energies studied in [3]. This was mostly due to high background counts at these energies where the reaction cross section falls off steeply. The background is made up of three main components: (1) noise in the PMT of the scintillator, (2) β^+ decays from ^{13}N produced by ^{1}H(^{12}C,γ) and ^{2}H(^{12}C,n), and (3) β^- decays from ^{24}Na produced by ^{13}C(^{12}C,p). The hydrogen exists in the target as a contaminant and also comes from residual gases in the vacuum system which collect on the target over time depending on the amount of beam and level of vacuum in the system (for more details see, for example, Ref. [11]). The ^{13}C was naturally present in the graphite target at a level of 1.1%. The amount of ^{24}Na activity ($t_{1/2}$ = 15 hrs) had built up from the previous higher-energy runs, but only became significant for the lowest energies. Since the presentation of this work at NN2012, attempts have been made to reduce the background level by using a highly-ordered pyrolytic graphite (HOPG) target, which is known to have low hydrogen contamination and successfully used in [9] for studying ^{12}C(^{12}C,p) at extreme sub-barrier energies. Also, the background from ^{24}Na was eliminated by using only low-energy ^{12}C beams on the target. By improving the background due to hydrogen and ^{13}C, the measurement was pushed down to 3.3 MeV. With a low-noise detector, the measurement will be able to go even lower. The next step will be to implement this technique with improvements using NSL's new 5 MV high-current accelerator. This combined with the neutron measurements presented in section 4 will provide a very clear picture of the strength of this reaction channel at stellar energies.

3. Low-energy extrapolation

Even a perfectly-designed experiment will suffer eventually from the steep drop-off of the reaction cross section at low energies, requiring longer and longer run times in order to achieve sufficient statistics. Since accelerator time is usually a limiting factor, one often has to give up at a certain energy after the cross section drops too low for the detection system to record enough events in a reasonable amount of time. Quite often this occurs well above the energy range interesting

for astrophysical applications. Therefore, it is necessary to determine a reliable extrapolation of the experimental data down to the lower energies of interest.

The extrapolation used for ^{12}C(^{12}C,n) in stellar models was provided by [3] (Fig. 3). As mentioned in the introduction, it is based on a Hauser-Feshbach statistical model calculation where the actual calculation overpredicted the cross section by a factor of 3, so the curve was renormalized to fit the baseline of the experimental data. The curve does seem to match the overall trend, but it clearly misses wherever resonances exist. Based on lower energy measurements in the proton and alpha channels [6, 8, 9], one might expect that resonances exist in the neutron channel in the unmeasured energy range. The question is if they are strong enough to enhance the reaction rate significantly over the rate based on the statistical model extrapolation. To date, no theory has successfully described the resonances observed in the ^{12}C fusion system. However, it may be possible to use the existing experimental data at low energies for the mirror reaction ^{12}C(^{12}C,p)^{23}Na to ascertain the resonant structure in the ^{12}C(^{12}C,n)^{23}Mg excitation function at these corresponding lower energies. Since the charged-particle channels are generally easier to measure, this could potentially provide a probe for investigating the absolute lowest energies relevant for the neutron channel. In formulating a prediction based on the ^{12}C(^{12}C,p) data, it is important to consider a few things. 1) The products n_i+^{23}Mg and p_i+^{23}Na (where i designates the state populated in the fusion residue after neutron/proton evaporation from the compound nucleus) are exact mirror systems: the two daughter nuclides, ^{23}Na and ^{23}Mg, are mirror nuclei having identical low-lying structure, so any fusion enhancement (or hindrance) due to entrance channel effects will show up equally well in both evaporation channels. 2) One must account for the difference in penetrability through the Coulomb barrier for each particle since the proton is charged while the neutron is electrically neutral. 3) The phase space will be different between the two channels since the two daughter nuclides have different masses governed by the Coulomb energy difference. This results in the different Q-values for the two channels ($Q_n = -2.6$ MeV and $Q_p = +2.2$ MeV). An additional consequence is that there are more daughter states available in ^{23}Na for ^{12}C(^{12}C,p) for a given reaction energy than there

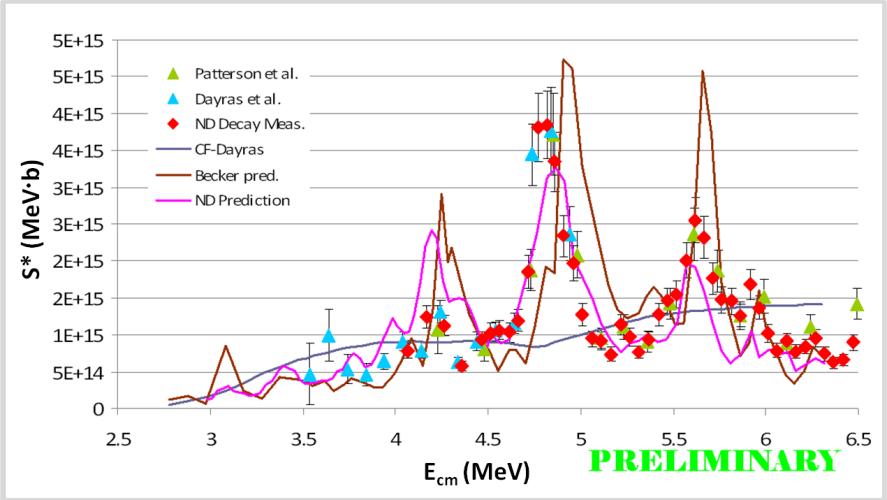

Figure 4. The predictions based on the data from [8] (——) and new data taken at NSL (——) are shown overlaid with the data from Fig. 3. The prediction associated with [8] has a systematic uncertainty of 30%. The systematic uncertainty of the NSL prediction has not been precisely determined but is of similar magnitude. The question of the existence of a resonance at 3.1 MeV is of key importance.

are in ^{23}Mg for ^{12}C(^{12}C,n). These extra states must be removed from consideration, since they do not contribute in the neutron channel, and the appropriate channels in ^{23}Na must be closed off at the same energies at which they close in the neutron channel. Taking all this into consideration and calculating the effects due to the penetrability and phase space differences, one should be able to formulate an accurate prediction of the neutron channel based on data from the proton channel (assuming the data is accurate). For the calculation of the penetrability and phase space effects, the statistical model code EMPIRE [13] was used to calculate the ratio n_i/p_i as a function of reaction energy. The resulting predictions are shown in Fig. 4 based on digitized data from [8] and data taken at NSL. The details of the NSL experiment are discussed in another paper within this conference proceedings [14]. One sees that the general structure is reproduced by the predictions in that all resonances are accounted for. However, the strengths of the resonances differ as well as the locations. This may be an artifact of the digitization of the graphical representation of the data from [8] or a real discrepency in normalization and energy determination between the two measurements (see Ref. [7]). Nevertheless, improved experimental data is needed in order to formulate a reliable prediction. The discrepancy brings into question the strengths of the low-energy resonances in the unmeasured energy range, in particular the potential resonance at 3.1 MeV which may contribute to the reaction rate at shell-carbon burning temperatures.

4. Neutron Detection

In a very recent experiment at NSL, the ^{12}C(^{12}C,n) reaction cross section was measured by direct detection of the outgoing neutron. This experiment took advantage of a highly efficient ^{3}He detector array surrounding the target (Fig. 5). The array consisted of twenty ^{3}He proportional counters embedded in a block of polyethylene in two concentric rings surrounding the target flange. The beam production was the same as described in Sec. 2, except only gas-stripping was used at the tandem terminal since the measurement focused primarily on the low-energy cross section. Only the 2^+ charge state of ^{12}C was selected since this was the most dominant product in this beam energy range, with typical beam currents of 1 pμA reaching the target. As in the ^{23}Mg decay measurement, it was necessary to consider the background components for the neutron detection measurement. Again, hydrogen contamination was a potential problem since ^{2}H(^{12}C,n)^{13}N also produced neutrons. Since the ^{3}He counter requires thermalization of neutrons for a non-negligible detection probability, all neutron energy information is lost and the ^{2}H(^{12}C,n) neutrons are indistinguishable from the ^{12}C(^{12}C,n) neutrons. This is also true for neutrons coming from ^{13}C(^{12}C,n)^{24}Mg which turned out to be quite a significant background

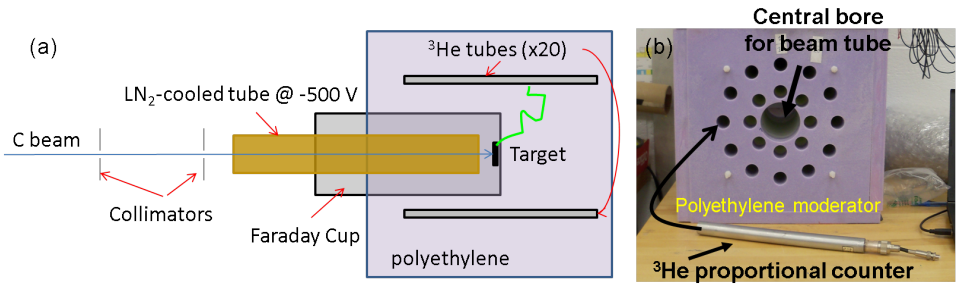

Figure 5. A schematic of the setup for the neutron detection measurement (a) and a picture of the polyethylene block with one ^{3}He proportional counter (b). The polyethylene has twenty small bores in two concentric rings for holding the ^{3}He counters around the target flange contained within the large central bore.

component. The remaining background neutrons came from the surrounding environment which were apparently products of cosmic ray interactions.

The hydrogen contamination in the target was rather well-controlled by the use of a HOPG target (see end of Sec. 2). To prevent build-up of contaminant hydrogen from the residual vacuum gases, a long copper tube cooled by liquid nitrogen was placed just in front of the target extending upstream to a 6 mm diameter collimator. An additional collimator, 12 mm in diameter, was placed further upstream which geometrically constrained the beam to the central portion of the target. The cold tube was charged to a potential of -500 V to prevent secondary electrons from escaping the target which formed part of a Faraday cup for reading the beam current. With this configuration, hydrogen contamination was not a limiting factor in the ^{12}C(^{12}C,n) cross section measurement.

To account for neutrons produced by ^{13}C(^{12}C,n), a ^{13}C beam was used to bombard the HOPG target through a range of energies corresponding to the appropriate center-of-mass energies used for the ^{12}C+^{12}C measurement. After correcting for the natural abundance of ^{13}C in the HOPG and for the difference in lab energy between the two beams within the thick target, the measured yield was converted to the yield due to ^{13}C(^{12}C,n) as a function of ^{12}C beam energy. This yield was then subtracted from the total leaving only the neutron yield due to ^{12}C(^{12}C,n).

A number of room background runs were taken throughout the course of the experiment and were found to be consistent, with the total rate (full array) determined as 9.01±0.09 neutrons/min. These runs were used to make the final background correction to the thick target neutron yield data. The corresponding cross section is proportional to 1) the derivative of the yield curve, which was obtained numerically, 2) the stopping power, which was calculated using SRIM [15], and 3) the detection efficiency, which was estimated using a Geant4 simulation. The resulting S* factor is shown in Fig. 6. The statistical uncertainty at the lowest energy plotted is 25%. Even lower energies were measured, however the beam-induced yields were consistent with a flat background—possibly due to deuterium on the beam line components or small amounts on the target. Unfortunately, the beam current produced by the tandem was

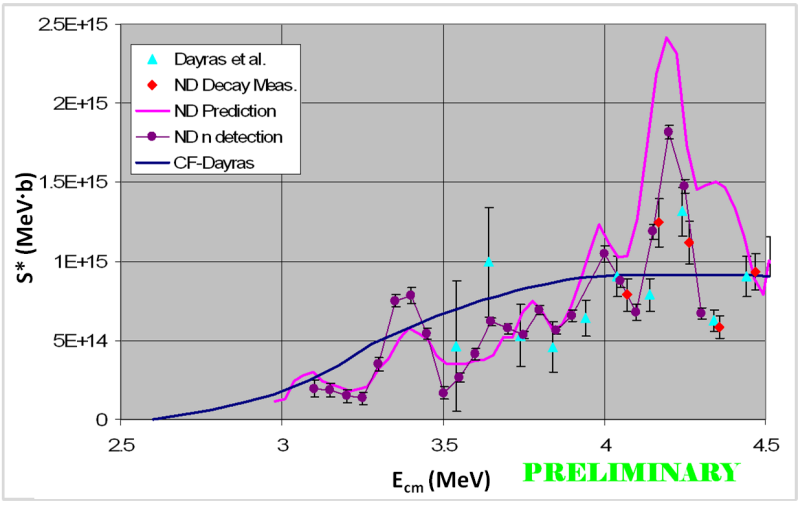

Figure 6. The low-energy portion of the excitation function is shown with the new data from the neutron detection measurement at NSL (●), along with data from Sec. 2 (♦), the data (▲) and extrapolation (——) from [3], and the NSL prediction from Sec. 3 (——). The new data agrees well with the other data sets in the overlapping region and extends to much lower energies. The NSL prediction continues to do well down to these lowest energies.

not sufficient to provide an unambiguous answer for this within the allotted beam time, but the data is still under analysis. Nevertheless, the neutron measurement yielded much lower-energy cross section measurements than the ^{23}Mg decay measurement, though there is more room for improvement in the decay measurement. This measurement represents the first to directly measure the cross section of ^{12}C(^{12}C,n) at astrophysical energies. Even more noteworthy is the good agreement between the new experimental data and the prediction provided in the previous section. In particular, the resonance at 3.4 MeV, which was predicted based on both the p_0 and p_1 channels, is also observed in the neutron channel. Current efforts are being made to confirm these results using the independent ^{23}Mg decay technique with the improvements mentioned in Sec. 2.

5. Astrophysical Implications

In discussing the astrophysical implications, it is first worth noting an important discrepancy in the neutron branching ratio provided in [3]. As mentioned in the introduction, Dayras et al. calculate the neutron branching ratio using a statistical model and then renormalize it to fit their data. These results are presented in Table 3 of [3] and have been used in combination with the total ^{12}C fusion S* recommended in [12] to form the ^{12}C(^{12}C,n) extrapolation plotted in Figures 3 and 4 (labeled as "CF-Dayras" in the legend). However, Dayras et al. go on to calculate the neutron branching ratio for various temperatures (Table 4 of [3]) and then provide an empirical formula with parameters to fit their calculations (Eq. 8 of [3]). In order to accurately fit the entire temperature range, two formulas are provided: one for temperatures above $T_9 = 1.5$ and another for lower temperatures. It is these formulas which were used in the model of [10] that produced Fig. 1 of this paper. But if one compares the low temperature formula with the numbers in Table 4 of that paper, a discrepancy is found (Fig. 7a). Apparently the fit parameters provided in Eq. 8 for the low-temperature formula are incorrect, resulting is an underestimation of the reaction rate for temperatures $1.0 < T_9 < 1.5$ and an overestimation of the rate for $T_9 < 1.0$ (Fig. 7b). For typical carbon-shell burning temperatures ($T_9 \simeq 1.1$), the corrected Dayras et al. rate is only 50% larger than the rate obtained by using Eq. 8a, but is more significant for slightly higher temperatures (350% at $T_9 = 1.4$). For a consistent comparison, however, we use the uncorrected rate derived from Eq. 8 in the discussion below since this represents the final recommendation of [3], and this is what was used to generate the abundances shown in Fig. 1.

As for the astrophysical implications of the new data, the predicted resonance at 3.1 MeV

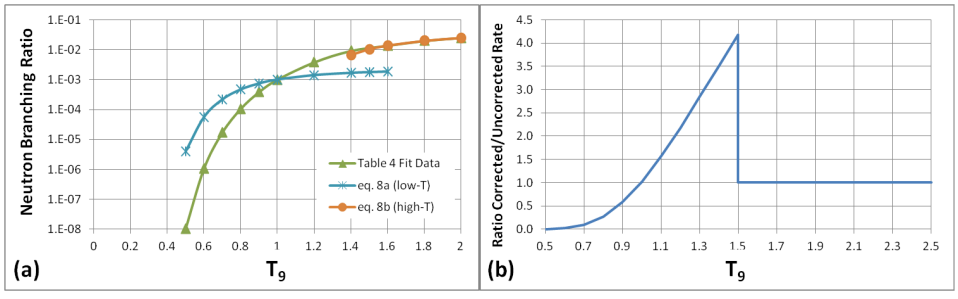

Figure 7. (a) shows the fit values for the neutron branching ratio provided in Table 4 of [3] (▲) with the values generated using Eq. 8a (∗) and Eq. 8b (●). Apparently Eq. 8a was published with wrong fit parameters. The correct parameters can be obtained by fitting the data labeled "this exp" in Table 4 and the ratio between the corrected equation and published equation is shown in (b).

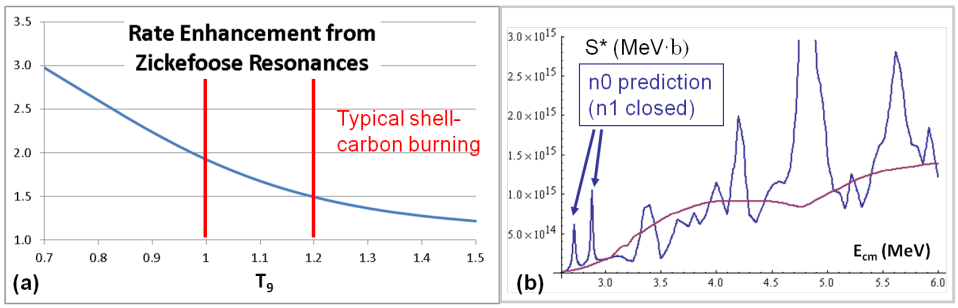

Figure 8. The curve in (a) represents the rate enhancement of ^{12}C(^{12}C,n) due to two low-energy resonances observed by [9] in the proton channel. The translation to the neutron channel is done following the prescription described in Sec. 3 and summing them on top of the smooth calculation produced by [3] (b). Even after assuming the maximum possible strength in the neutron channel, these resonances only contribute marginally for typical shell-carbon burning temperatures ($1.0 < T_9 < 1.2$).

based on the data from [8] has not been confirmed, though this lies at the limit where the background becomes more uncertain. Instead, the measured S* factor seems to follow the trend predicted from the proton measurements at NSL. Without a strong resonance at 3.1 MeV as suggested by the Becker et al. data, the real astrophysical rate will not likely exceed the uncorrected Dayras rate for weak s-process scenarios, unless there is a significant enhancement coming from the lower energies. To estimate the maximum possible contribution from this region, we consider two things. 1)The CF-Dayras *S* factor* appears to overestimate the non-resonant component of the excitation function, particularly at the lowest energies where only the very peaks of the resonances lie above it (Fig. 6). We take this as the baseline for our estimation. 2)To estimate the resonant structure, we follow the procedure outlined in Sec. 3. At these low energies, it is only n_0 which contributes since n_1 closes at 3.05 MeV. To formulate a prediction in n_0, a measurement of ^{12}C(^{12}C,p_0) is needed. There is only one available data set covering sufficiently low energies [9]. In that measurement, they used a high intensity ^{12}C beam on a thick HOPG target and measured the p_0 and p_1 protons with two large-solid angle silicon detector telescopes at 135°, but were unable to distinguish between the two proton groups. The combined (p_0+p_1) thick target yield was recorded with the goal of searching for low-energy resonances that may be important in various astrophysical scenarios. Resonances were identified and their parameters extracted based on the shape of the thick target yield curve. Two resonances between the energies of 2.6 and 3.0 MeV were identified in that study. To estimate the maximum contribution of these resonances in the neutron channel, we assume the full strength of each comes from the p_0 channel, since any strength from p_1 corresponds to strength in n_1 which is closed in this energy range. Then the predicted neutron resonances are added on top of the CF-Dayras baseline. In this way, a confident qualitative upper limit can be established, since both the resonant and non-resonant components are seemingly overestimated. Using this new extrapolation, the reaction rate enhancement is still less than twice the uncorrected Dayras rate at normal shell-carbon burning temperatures (Fig. 8). Then based on the study by Pignatari [10] (Fig. 1), one can postulate that the change in carbon-shell abundances due to the uncertainty in the ^{12}C(^{12}C,n) rate is quite minimal for Population I massive stars.

6. Conclusions

Though ^{22}Ne(α,n) is expected to be the main source of neutrons in the weak s-process, the uncertainty in the low-energy ^{12}C(^{12}C,n) cross section has facilitated the possibility of this

reaction contributing a large neutron flux which could significantly alter the heavy element abundances produced in this scenario. The large uncertainty arises due to the rich resonant structure present across the whole sub-barrier excitation function down to the lowest measured energies. Furthermore, this reaction has not been well-studied to date, and experimental data ends at relatively high energies compared with the energies of astrophysical interest. For these energies, stellar models must rely on a dubious extrapolation based on a renormalized statistical model calculation. The aim of this work was to provide additional experimental data to confirm the results of [3] and [4] and extend the data to lower energies towards the range of astrophysical relevance as well as provide a more reliable extrapolation in the lowest range inaccessible by experiments. To a degree, these goals have been met. The new experimental data provided in this study has good agreement with the literature data and has successfully reached much lower energies—down to 3.10 MeV, from the previous lowest 3.54 MeV, where the cross section drops by more than a factor of 20. The new data set provides the first direct measurements at energies important for astrophysical scenarios such as the weak s-process and explosive carbon burning. To cover the lower unmeasured energies, a more reliable extrapolation technique has been formulated based on measurements of the mirror reaction channel ^{12}C(^{12}C,p) which has been successfully measured at lower energies in [9]. This extrapolation technique has been proven to be more reliable than the statistical model calculation provided in [3] by comparison with experimental data. This combined with the new experimental data considerably reduces the uncertainty in the low-energy cross section where it is now expected that any reaction rate enhancement due to unmeasured resonances should be less than a factor of 2 over the rate derived from [3] for shell-carbon burning temperatures. Given this enhancement limit, 1-D models of massive Population I stars predict a minimal change in heavy element abundances produced during shell-carbon burning.

7. Acknowledgements

The authors are grateful to F. Montes and H. Schatz for their contribution of three proportional counters which completed the full set of twenty allowed for the detector array, and to M. Wiescher for his continued guidance and support for this project. This work was supported by the National Science Foundation under Grants No. PHY-0758100 and No. PHY-0822648, the National Natural Science Foundation of China under Grant No. 11021504, and the University of Notre Dame.

References

[1] Pignatari M, Gallino R, Heil M, Wiescher M, Käppeler F, Herwig F and Bisterzo S 2010 *Astrophys. J.* **710** 1557
[2] Longland R, Iliadis C and Karakas A I 2012 *Phys. Rev.* C **85** 065809
[3] Dayras R A, Switkowski Z E and Woosley S E 1977 *Nucl. Phys.* A **279** 70
[4] Patterson J R, Winkler H and Zaidins C S 1969 *Astrophys. J.* **157** 367
[5] Notani M *et al.* 2012 *Phys. Rev.* C **85** 014607
[6] Spillane T *et al.* 2007 *Phys. Rev. Lett.* **98** 122501
[7] Aguilera E F *et al.* 2006 *Phys. Rev.* C **73** 064601
[8] Becker H W, Kettner K U, Rolfs C and Trautvetter H P 1981 *Z. Phys.* A **303** 305
[9] Zickefoose J 2010 Ph.D. thesis University of Connecticut
[10] Pignatari M 2011 private communication
[11] Aguilera E F, Rosales P, Martinez-Quiroz E, Murillo G and Fernández M C 2006 *Nucl. Instr. and Meth.* B **244** 427
[12] Caughlan G R and Fowler W A 1988 *At. Data Nucl. Data Tables* **40** 283
[13] Herman M, Capote R, Carlson B V, Obložinský P, Sin M, Trkov A, Wienke H and Zerkin V 2007 *Nucl. Data Sheets* **108** 2655
[14] Fang X *et al.* this conference proceedings
[15] Ziegler J F 2012 www.srim.org